



Contents lists available at ScienceDirect

International Journal of Mechanical Sciences

journal homepage: www.elsevier.com/locate/ijmecsci

Closed-form equation for natural frequencies of beams under full range of axial loads modeled with a spring-mass system

Juan Valle^{a,*}, Daniel Fernández^b, Jordi Madrenas^a

^a Department of Electronic Engineering, Universitat Politècnica de Catalunya, Barcelona, Spain

^b Nanusens, Barcelona, Spain

ARTICLE INFO

Keywords:

Axial load

Beam

Equation

Lumped model

Natural frequency

Vibration

ABSTRACT

A new simple closed-form equation that accurately predicts the effect of an arbitrarily large constant axial load, residual stress or temperature shift on the natural frequencies of a uniform single-span beam, with various end conditions, is presented. Its accuracy and applicability range are studied by comparing its predictions with numerical simulations and with the approximate Galef's and Bokaian's formulas. The new equation may be understood as a refinement or extension of these two approximate formulas. Significant accuracy and applicability range improvements are achieved, especially near the buckling point and for large and moderate axial load. The new closed-form equation is applicable in the full range of axial load, i.e., from the buckling load to the tensioned-string limit. It also models well the beam-to-string transition region for the eight boundary conditions studied. It works remarkably well in the free-free and sliding-free cases, where it is a near-exact solution. In addition, it yields the natural frequencies of a 1-D spring-mass system that may be used to model tensioned beams, and potentially, more complex systems.

1. Introduction

The study of the vibration of beams subjected to axial loads is a classic topic discussed in many technical publications [1–19]. One reason for this is that the natural frequencies of axially loaded beams, widely used in many macro and micro structures, are of practical interest in a large number of applications. For example, for structural health monitoring of structures [18–20]; for using resonance as a sensing mechanism in micro and nano-devices [21]; for predicting the behavior of micro devices under temperature or stress variations [22,23]; for estimating the tension, residual stress and other physical parameters from the vibration response [18,19,24]; and in general for analyzing free vibrations of any other beam-type tensioned or compressed structure.

The natural frequencies of beams under no axial load can be calculated with very well known analytical formulas [25]. However, an axial load has the effect of increasing the natural frequency if the load is tensile, or decreasing it if the load is compressive. At a critical compressive load P_{cr}^i the frequency goes to zero and the beam buckles. Contrarily, if the beam is sufficiently tensioned, the flexural rigidity EI is insignificant compared to the bending stiffness associated with the applied tension. The beam behaves as a straight tensioned string in this latter case. Given that, in many situations, beams are subjected to temperature shifts or axial loads, or are fabricated with non-zero axial residual stress, important shifts in their natural frequencies may be observed. This can be seen, for

example, in [26], where the beam-to-string transition of axially loaded carbon nanotubes was characterized. In this regard, an approximate simple equation for predicting natural frequency as a function of axial load for clamped-clamped beams was proposed by Galef in 1968 [1]. It established a linear relationship between the squared frequency ω^2 and the axial load T . Later, Bokaian [3,4] showed that this relationship is exact for three types of boundary conditions [3,9] (pinned-pinned, sliding-sliding, and sliding-pinned single-span uniform beams). The problem is explicitly solvable in those 3 particular cases because the vibration mode shape under no axial load and the buckling mode shape are identical [4,27], which does not occur in general. Interestingly, Guédé et al. [5] then showed that there are some very special cases of inhomogeneous beams where those formulas also hold. When the axial load is not larger than the buckling load, the accuracy of Galef's equation is generally within 1% (see 8.1.4 of [25]). However, in the case of larger axial loads, very common in micro and nano-beams [26], its accuracy can be worse than 10%. In 1989, Joshi [6] added a quadratic term to Galef's equation in order to improve its accuracy between -0.4 and 2.0 times the buckling load. Unfortunately, for larger loads the error of the quadratic equation grows significantly. Bokaian [4] then suggested a modified Galef's formula with a corrective coefficient which depends on the type of end conditions, increasing its applicability to other end conditions. Liu et al. [10] focused on the free-free beam and calculated numerically the natural frequencies ω as a function of the applied tension

* Corresponding author.

E-mail addresses: juanvallefraga@gmail.com (J. Valle), daniel.fernandez@nanusens.com (D. Fernández), jordi.madrenas@upc.edu (J. Madrenas).

<https://doi.org/10.1016/j.ijmecsci.2019.02.014>

Received 13 July 2018; Received in revised form 27 January 2019; Accepted 11 February 2019

Available online 14 February 2019

0020-7403/© 2019 The Authors. Published by Elsevier Ltd. This is an open access article under the CC BY license. (<http://creativecommons.org/licenses/by/4.0/>)

T. Then, they obtained by least-squares fitting several cubic polynomial equations that relate ω and *T* for the first 4 modes. However, a cubic equation does not describe well the behavior over a wide range of axial load. For this reason, depending on whether the axial load was small, medium or large, the resonance frequency had to be looked up using a plot, or one of the two sets of cubic equations given in the article.

In some cases, the practical applications deal with highly tensioned structures. In this regard, estimation of cable tension from its natural frequencies using approximate simple formulas rather than iteration or numerical processes has been the objective of several works [15–19]. Many of them include the effects of flexural rigidity and/or cable sag. Flexural rigidity cannot be neglected when tension is sufficiently small. While gravity effects are negligible in the microscopic world they need to be considered in long macroscopic cables used, for example, in bridges [28]. In [15] several approximate formulas for calculating the first and second natural frequencies of inclined cables are provided. They work well but, similarly to [10], each formula is applicable for a different positive tension range. Mehrabi and Tabatabai [16] proposed a similar non-dimensional relationship than worked well for clamped-clamped conditions and tension values over a given threshold. Ren et al. [17] proposed empirical expressions when considering either bending stiffness or cable sag. Again, each expression is applicable for a given range of tensile axial load. Fang et al. [18] derived by curve-fitting a simple explicit formula for calculating the natural frequencies of axially tensioned cables, which takes into account bending stiffness but cable sag is ignored. It works well for relatively high tension values and higher or antisymmetric vibration modes of clamped-clamped cables where the bending stiffness cannot be neglected. In 2015, Huang et al. [19] explicitly presented unified practical formulas for three types of boundary conditions, namely, pinned-pinned, clamped-clamped and pinned-clamped ends. Cable tension may be calculated using frequencies of the first 10 modes. Bending stiffness is accounted for, but cable sag is considered negligibly small. Fortunately, the second or higher modes may be used to calculate tension in cables with large sag extensibility [18]. Another benefit of these unified formulas is that they are continuous rather than piecewise functions. However, the calculation of the parameter of the unified formulas is not trivial and typically requires numerical procedures. In addition, although they work well for most cable-stayed bridges, they will not work well for axially loaded structures where the axial load is sufficiently small or compressive. This limitation is shared by the other aforementioned formulas applicable for tensioned cable structures [15–19]. In addition, most of them use piecewise functions based on the tension or frequency value. Finally, either clamped-clamped conditions are assumed, or numerical procedures or different formulas are required to find the relation between tension and frequency.

Additionally, more complex axially loaded systems have been and still are the focus of extensive research. Some examples include non-uniform initial stress in curved beams, studied in [29], which derived the equations of motion using the principle of virtual work. Recently, the effects of initial curvatures on the fundamental frequency of axially loaded beams were studied experimentally and numerically in [13]. Coupled flexural-torsional vibration in the presence of axial loads was studied, for example, in [6,30], while axial-bending coupled vibration was studied in [31]. Furthermore, [32,33] considered non constant axial forces and [33,34] included an added mass. The presence of cracks in axially loaded beams has also dragged the attention of researchers, such as in [35–39]. Many studies [12,14,31,37,38,40–44] tackled the problem of modeling general loads, arbitrary boundary conditions or geometric discontinuities, such as cracks or multi-span beams, by making use of attached lumped elements, such as springs, spring-mass systems, dampers and others. Other studies, such as [31,45–47] focused on, or considered, forced vibrations of axially loaded beams. Recently, [31] presented an analytical method for solving both free and forced vibrations of axially loaded stepped multi-layered beams with arbitrary boundary conditions. Nonlinear behavior of axially loaded beams was

treated mathematically, for example, in [34,48,49]. More specifically, Gunda et al. [49] derived approximate closed-form solutions that relate resonance frequency with vibration amplitude, useful when the vibration amplitude is large enough to cause membrane stretching of the beam, and its associated nonlinear behavior. Experimental studies were also conducted in [50] to measure the natural frequency of a clamped-clamped steel beam under large axial tensile force, reaching the plastic deformation regime. [51] derived an analytical solution for the free vibration of simply supported axially loaded nanobeams based on non-local elasticity theory, rather than classical continuum theory. Finally, [46] recently developed an energy finite element method for predicting the high frequency vibration response of beams with axial force. Evidently, the research of axially loaded beams is broad and still intense.

The recent advances in numerical and analytical methodologies have provided very useful tools for dealing with increasingly complex axially loaded systems. For example, the characteristic frequency equation of complex systems may be obtained using relatively laborious methodologies. But the resonance frequency is still contained in a transcendental equation, only solvable numerically as in [52]. So, despite of all the previous work, there is no explicit equation that provides accurate resonance frequency estimation for the full range of axial load, i.e. from the buckling load to the string limit regime, with other end conditions apart from the three types previously mentioned. As a consequence, and given their simplicity, Galef's [1] and Bokaian's equations [4] are still widely used as in [20,22,23,26,53].

In this study we search for a generic explicit and simple closed-form equation that accurately predicts natural frequencies of beams as a function of the axial load, temperature variation or residual stress, valid for general boundary conditions, and from the buckling point to the string limit regime. The formula will be obtained in Section 2.5 after adding a correction term to Bokaian's equation. Empirical coefficients will be calculated analytically for the fundamental mode, and numerically for the first 5 vibrational modes using eight different boundary conditions.

Lumped models play a very important role in current physical system modeling. For this reason, a simple spring-mass system that models the natural frequencies of axially loaded beams will be also provided in Section 2.5.

2. Analytical formulation

2.1. Background

Two well-known methods for studying the mechanical vibration of continuous systems are: 1) Direct solving of the related differential equations and 2) Rayleigh's method or energy approach. Let us briefly discuss both methods applied to axially loaded beams.

2.2. Direct solving of the equations

Under the assumption that the material is linearly elastic, and the shear deformation and rotary inertia are negligible (Euler–Bernoulli beam theory), the equation of motion that governs the small deflection *Y* of an axially loaded beam as a function of the position *x* and time *t* is the following linear partial differential equation ([2,54]):

$$\frac{\partial^2}{\partial x^2} \left(EI(x) \frac{\partial^2 Y(x,t)}{\partial x^2} \right) - \frac{\partial}{\partial x} \left(\sigma A \frac{\partial Y(x,t)}{\partial x} \right) + \rho A \frac{\partial^2 Y(x,t)}{\partial t^2} = q(x,t) \quad (1)$$

where $q(x, t)$ is the external transversal force per unit length (a list of symbols is given in the Appendix B). The effect of the axial load is contained in the second term, which if moved to the right hand side, may be interpreted as the transversal force that appears when an axial load or tension $T = \sigma A$ is applied to the beam. For constant tension along the beam, this force is directly proportional to the second derivative of *Y*, or the beam curvature ($\partial^2 Y / \partial x^2$).

For the free vibration case ($q(x, t) = 0$), and assuming constant tension along the beam ($\partial(\sigma A) / \partial x = 0$) and a sinusoidal dependence of dis-

placement with time $Y(x, t) = Y(x) * \sin(\omega t)$ Eq. (1) yields:

$$\frac{d^2}{dx^2} \left(EI(x) \frac{d^2 Y(x)}{dx^2} \right) - \sigma A \frac{d^2 Y(x)}{dx^2} - \rho AY(x)\omega^2 = 0 \quad (2)$$

The solution of Eq. (2) involves solving a transcendental characteristic equation as shown in [4,9,10]. Although numerically solvable, transcendental equations often do not have analytical closed-form solutions. Galef [1] and later Bokaian [4] proposed simple closed-form equations for describing the approximate variation of the normalized natural frequency parameter, $\bar{\Omega}$ with the normalized tension parameter \bar{U} . Both equations will be discussed in the following sections.

2.3. Rayleigh’s method

The resonant frequency of a mechanical system can be also obtained by equating its maximum kinetic energy to its maximum potential energy. This procedure is known as the Rayleigh energy method and, for the case of mechanical beams when the exact modal shape $Y(x)$ is known, the obtained frequency is exact. Otherwise, it is an approximation. Typically, the final expression has the system’s effective stiffness in the numerator and an effective mass in the denominator. For example, as stated in [4], the Rayleigh quotient for the fundamental natural frequency ω of a beam with axial tension T may be written as:

$$\omega(T) = \left(\frac{\int_0^L EI(d^2 Y/dx^2)^2 dx + T \int_0^L (dY/dx)^2 dx}{\int_0^L \rho AY^2 dx} \right)^{1/2} \quad (3)$$

Y typically depends on the applied load T , so its exact calculation involves solving Eq. (2) and its associated transcendental equation, which unfortunately does not allow a closed-form solution for the frequency as a function of the applied tension. For this reason, significant effort [1–7,10] has been put into finding and analyzing simple closed-form equations that describe the variation of ω with the applied tension.

2.4. Lumped 1-D model description

Let’s multiply the numerator and denominator of Eq. (3) by $1/Y_{max}^2$ and rewrite it in terms of the effective stiffness and mass, yielding:

$$\omega(T) = \left(\frac{K_B(T) + K_T(T)}{M(T)} \right)^{1/2} = \left(\frac{K_B(T)}{M(T)} \right)^{1/2} \cdot \left(1 + \frac{K_T(T)}{K_B(T)} \right)^{1/2} \quad (4)$$

which corresponds to a 1-D mechanical system composed of a mass $M = \int_0^L \rho AY^2 dx$ connected to two springs in parallel, $K_B = \int_0^L EI(d^2 \bar{Y}/dx^2)^2$ or flexural stiffness, and $K_T = T \int_0^L (d\bar{Y}/dx)^2 dx$ or tensional stiffness (see Fig. 1).

If Y were independent of the applied tension, as is the case for pinned-pinned, sliding-sliding and pinned-sliding beams (see [4]), M and K_B would be constant and K_T directly proportional to the applied tension. Therefore, ω^2 would be linearly dependent on the applied tension T and the following equation, known as Galef’s equation [1], would

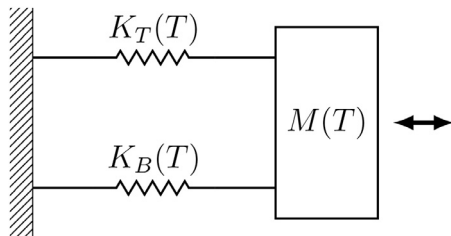


Fig. 1. Spring-mass system that models the natural frequency of an axially loaded beam. Total stiffness is $K(T) = K_B(T) + K_T(T)$, where $K_B(T)$, $K_T(T)$ and $M(T)$ can be interpreted as the bending stiffness, tension-induced stiffness and the system’s effective mass, respectively.

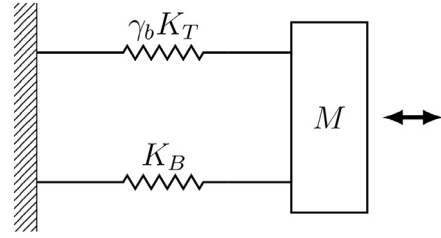


Fig. 2. Spring-mass system that models the natural frequency predicted by Bokaian’s equation. Total stiffness is $K = K_B + \gamma_b K_T$, and the dependence on the applied tension remains only in K_T , being K_B , M and γ_b constant parameters. It is exact when the shape of the deformed beam is independent of the applied tension.

describe exactly the dependency of the resonant frequency on T :

$$\omega(T) = \omega_0 \left(1 + \frac{K_T(T)}{K_B} \right)^{1/2} = \omega_0 \left(1 + \frac{T}{P_{cr}} \right)^{1/2} \quad (5)$$

where $\omega_0 = (K_B/M)^{1/2}$ is the natural frequency when no axial load is applied and P_{cr} is the critical buckling load. The previous equation can be rewritten as:

$$\bar{\Omega} = (1 + \bar{U})^{1/2} \quad (6)$$

where \bar{U} is the normalized tension parameter, which like K_T , is also proportional to T . Note that when $K_T = -K_B$ both the stiffness and frequency are zero which, by definition occurs when $\bar{U} = -1$ or, equivalently, $T = -P_{cr}$.

Unfortunately, Eq. (5) does not hold when Y depends on the applied tension. Bokaian [4] tackled this problem by introducing a new coefficient called γ_b into Eq. (5), in order to approximately account for the dependence with tension (see Eq. (7)). The beam end conditions determine entirely the value of γ_b , obtained in [4], where the modal shape of a beam with no axial load was assumed.

$$\omega(T) \approx \omega_0 \left(1 + \gamma_b \frac{K_T(T)}{K_B} \right)^{1/2} = \omega_0 \left(1 + \gamma_b \frac{T}{P_{cr}} \right)^{1/2} \quad (7)$$

Bokaian’s equation implicitly assumes that K_B and M are tension independent and K_T linearly dependent on T . The modified corresponding spring-mass system is depicted in Fig. 2.

Finally, Bokaian’s Eq. (7) can be rewritten in its most known form:

$$\bar{\Omega} = (1 + \gamma_b \bar{U})^{1/2} \quad (8)$$

This equation constitutes a simple upper bound approximation [4] to beams under tensile loads with different end conditions, whose effects are accounted for in the coefficient γ_b . Numerical simulations show that it is accurate (error $\leq 1\%$) for small positive axial loads ($\bar{U} \lesssim 1$), but does not work so well for medium or large ones ($\bar{U} \gtrsim 15 - -20$), where it typically has a $\sim 5-15\%$ error. For large axial loads, the beam behaves like a tensioned string and Bokaian proposed to use the well-known string solution ([25]) as a lower bound approximation to the natural frequency. Unfortunately, the transition between small axial loads and the string behavior at medium/large axial loads cannot be well described by any of the previous equations.

The main objective of this article is to provide a simple model or equation that predicts the natural frequency for a very large range of axial loads accurately, including compressive loads down to the buckling point ($\bar{U} = -1$) and the transition between low axial loads (flexural regime) and large axial loads (tensioned-string regime).

2.5. Correction term and new extended lumped 1-D model

The beam-to-string transition is governed by the relative importance of the first and second terms in Eq. (2). In order to model this transition,

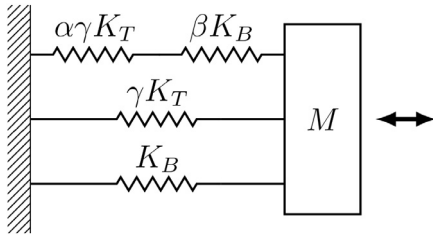


Fig. 3. Spring-mass system that models the natural frequency predicted by new closed-form equation, which includes the beam-to-string transition correction term. Total stiffness is $K = K_B + \gamma \cdot K_T + \frac{1}{\frac{1}{\alpha\gamma K_T} + \frac{1}{\beta K_B}}$. Tension dependence only appears in K_T , being the rest constant parameters.

let us introduce a correction term into Eq. (7) of the form:

$$\omega(T) \approx \omega_0 \left(1 + \gamma \frac{K_T(T)}{K_B} + \frac{1}{\frac{1}{\alpha\gamma \frac{K_T(T)}{K_B} + \frac{1}{\beta}}} \right)^{1/2} = \frac{\omega_0}{K_B^{1/2}} \left(K_B + \gamma K_T(T) + \frac{1}{\frac{1}{\alpha\gamma K_T(T)} + \frac{1}{\beta K_B}} \right)^{1/2} \quad (9)$$

whose associated spring-mass model is shown in Fig. 3. Again, as in Eqs. (6) and (8), the previous equation can be written in terms of \bar{U} and $\bar{\Omega}$, yielding the simpler form:

$$\bar{\Omega} \approx \left(1 + \gamma \bar{U} + \frac{1}{\frac{1}{\alpha\gamma \bar{U}} + \frac{1}{\beta}} \right)^{1/2} \quad (10)$$

The natural frequency of the axially tensioned system ω may be also written in terms of the natural frequency of the same system without axial load ω_0 , applied tension T and critical buckling load for mode i , P_{cr}^i , which can be found in Table 1 of [4], for example. For simplicity, all parameters are tabulated in Table 2 and Table A.3 in Appendix A:

$$\omega(T) \approx \omega_0 \left(1 + \gamma \frac{T}{P_{cr}^i} + \frac{1}{\frac{1}{\alpha\gamma \frac{T}{P_{cr}^i}} + \frac{1}{\beta}} \right)^{1/2} \quad (11)$$

As it will be shown in Section 3, the new correction term can accurately model the interaction between the first and second left-hand-side

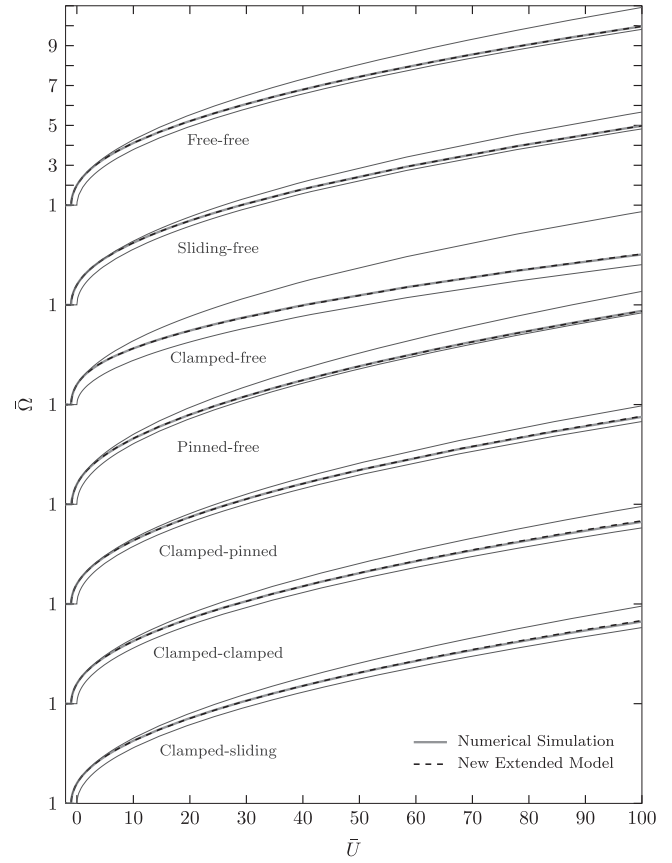


Fig. 4. Numerical simulation of the variation of normalized resonant frequency ($\bar{\Omega}$) with normalized tension (\bar{U}) in the first mode for several boundary conditions (gray), this study approximation (dashed), and its lower (tensioned-string) and upper bound (Bokaian) approximations (solid black thin lines).

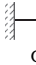
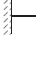


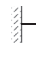

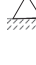

(LHS) terms of Eq. (2) and thus determine the transition characteristics from one regime to the other.

Writing the relationship between applied tension and resonance frequency as in Eqs. (9) and (11) has one worth-mentioning advantage: parameters α , β and γ are invariant in symmetrically equivalent systems. This invariance is shown explicitly in Table 1. The invariance will be confirmed in Section 3, where the 3 parameters will be calculated in the cases shown in Table 1.

Table 1
Symmetry equivalences. Two equivalent cases yield the same α , β and γ , and therefore are represented by the same Eq. (11).

Clamped-Sliding		Clamped-Clamped		Clamped-Pinned
Mode 1	≡	Mode 1		Mode 1
Mode 2	≡	Mode 2	≡	Mode 1
Mode 3	≡	Mode 3	≡	Mode 2
		Mode 4	≡	
		Mode 5		
Sliding-Free		Free-Free		Pinned-Free
Mode 1	≡	Mode 1		Mode 1
Mode 2	≡	Mode 2	≡	Mode 1
Mode 3	≡	Mode 3	≡	Mode 2
		Mode 4	≡	
		Mode 5		

Table 2
Analytic results for the 3 parameters of Eq. (10) for the fundamental mode, and accuracy comparison with Eqs. (6) (Galef's) and (8) (Bokaian's).

Boundary conditions	λ_1 U_{mi} Γ_i	γ_b \bar{P}_{cr}	Eq. (10) Derived Parameters α, β, γ	Max Error			
				$(-1 < \bar{U} < 1)$ tom		$(0 < \bar{U} < \infty)$	
				Eq. (10)	Eq. (6)	Eq. (10)	Eq. (8)
 Clamped-Clamped	4.73004074 $(i + 1)^2 \pi^2 / 2^*$ $i\pi\sqrt{2}$	0.970 1	$\gamma = 0.77839$ $\alpha = 0.24615$ $\beta = 1.4154$	0.17%	1.9%	2.06%	>10%
 Clamped-Sliding	2.36502037 $i^2 \pi^2 / 2$ $(2i - 1)\pi / \sqrt{2}$	0.970 1/4	$\gamma = 0.77839$ $\alpha = 0.24615$ $\beta = 1.4154$	0.10%	1.7%	2.06%	>10%
 Clamped-Pinned	3.92660231 $(2i + 1)^2 \pi^2 / 8$ $i\pi\sqrt{2}$	0.978 2.0457/4	$\gamma = 0.83796$ $\alpha = 0.16712$ $\beta = 1.0314$	0.15%	1.5%	1.47%	>7%
 Pinned-Pinned	π $i^2 \pi^2 / 2$ $i\pi\sqrt{2}$	1.000 1/4	$\gamma = 1.0000$ $\alpha = 0.0000$ $\beta = N/A$	<0.1%	<0.1%	<0.1%	<0.1%
 Clamped-Free	1.87510407 $(2i - 1)^2 \pi^2 / 8$ $(2i - 1)\pi / \sqrt{2}$	0.926 1/16	$\gamma = 0.49247$ $\alpha = 0.88033$ $\beta = 2.9734$	0.13%	4.0%	3.33%	>30%
 Free-Free	4.73004074 $i^2 \pi^2 / 2$ $(i + 1)\pi\sqrt{2}$	0.975 1/4	$\gamma = 0.77839$ $\alpha = 0.25258$ $\beta = 1.7427$	0.04%	1.4%	0.09%	>10%
 Pinned-Free	3.92660231 $i^2 \pi^2 / 2$ $(2i + 1)\pi / \sqrt{2}$	1.000 1/4	$\gamma = 0.92196$ $\alpha = 0.22586$ $\beta = -0.12488$	∞	∞	∞	>10%
 Sliding-Free	2.36502037 $(2i - 1)^2 \pi^2 / 8$ $i\pi\sqrt{2}$	0.975* $i\pi\sqrt{2}$ 1/16	$\gamma = 0.77839$ $\alpha = 0.25258$ $\beta = 1.7427$	0.08%	1.4%	0.12%	>10%

* $(i + 1)^2 \pi^2 / 2$ does not hold for mode 2. In turn, $U_{m2} = 8.18^2 \pi^2 / 2$, approximately. ** In [4] this is 0.925, but it should be 0.975.

2.6. Analytic derivation of α, β and γ

Parameters α, β and γ may be calculated analytically provided that 3 conditions are imposed to Eq. (10). Let us use the following ones:

Condition 1 With very large axial load ($\bar{U} \rightarrow \infty$) the beam must behave as a tensioned string or cable.

Firstly, let us rewrite the classic relations between f and T for tensioned strings in terms of $\bar{\Omega}$ and \bar{U} . According to [4] these may be put in the following form:

$$\frac{2\pi f L^2}{\alpha} = \Gamma_i \sqrt{\frac{TL^2}{2EI}} = \Gamma_i \sqrt{U} \tag{12}$$

where Γ_i is shown in column 18 of Table 1 in [4], and is also displayed in Table 2 of this work. On the other hand, the natural frequency of an unloaded beam is:

$$f_0 = \frac{\lambda_i^2}{2\pi L^2} \alpha \tag{13}$$

where λ_i can be found in page 108 of [25] or Table 2. Using Eqs. (12) and (13) it is now straightforward to write $\bar{\Omega}$ as a function of \bar{U} :

$$\bar{\Omega} = \frac{f}{f_0} = \frac{\Gamma_i}{\lambda_i^2} \sqrt{U} = \left(\frac{\Gamma_i^2}{\lambda_i^4} \cdot U_{mi} \cdot \bar{U} \right)^{\frac{1}{2}} \text{ (Classic string equation)} \tag{14}$$

Secondly, note that when $\bar{U} \rightarrow \infty$ Eq. (10) may be simplified to:

$$\bar{\Omega} = (\gamma \bar{U})^{\frac{1}{2}} \text{ (String limit of equation 10)} \tag{15}$$

Which shows that the behavior of Eq. (10) at very large axial load is solely determined by γ .

Finally, comparison of Eqs. (14) and (15) yields the value of γ :

$$\gamma = \frac{\Gamma_i^2}{\lambda_i^4} \cdot U_{mi} \tag{16}$$

Condition 2 With very small axial load ($\bar{U} \rightarrow 0$) the beam must behave as described by Bokaian's Eq. (8).

Firstly, note that when $\bar{U} \rightarrow 0$ Eq. (10) may be simplified to:

$$\bar{\Omega} = (1 + \gamma(1 + \alpha)\bar{U})^{\frac{1}{2}} \tag{17}$$

By comparing Eq. (17) with Bokaian's Eq. (8) the following correspondence can be made:

$$\gamma_b = \gamma(1 + \alpha) \tag{18}$$

And α may be found with the following relation:

$$\alpha = \frac{\gamma_b}{\gamma} - 1 \tag{19}$$

Condition 3 Resonance frequency must be zero ($\bar{\Omega} = 0$) at the buckling load ($\bar{U} = -1$).

Note that this important condition is met by Galef's Eq. (6) but not so by Bokaian's Eq. (8). In our case, making $\bar{\Omega} = 0$ at $\bar{U} = -1$ in Eq. (10) yields:

$$\beta = \frac{1}{\frac{1}{\alpha\gamma} + \frac{1}{\gamma-1}} = \frac{(\gamma-1)(\gamma-\gamma_b)}{1-\gamma_b} \tag{20}$$

where the relation (19) has been used to express β as a function of γ and γ_b .

3. Result comparison and discussion

Numerical simulations were performed to obtain the frequency versus applied tension curves for the same boundary conditions considered in Bokaian's works [3,4]. To this end, a very long and thin beam ($L/t = 10000$) was simulated using a quadratic three-node beam element in 3-D (BEAM189) from commercial finite-element software ANSYS®.

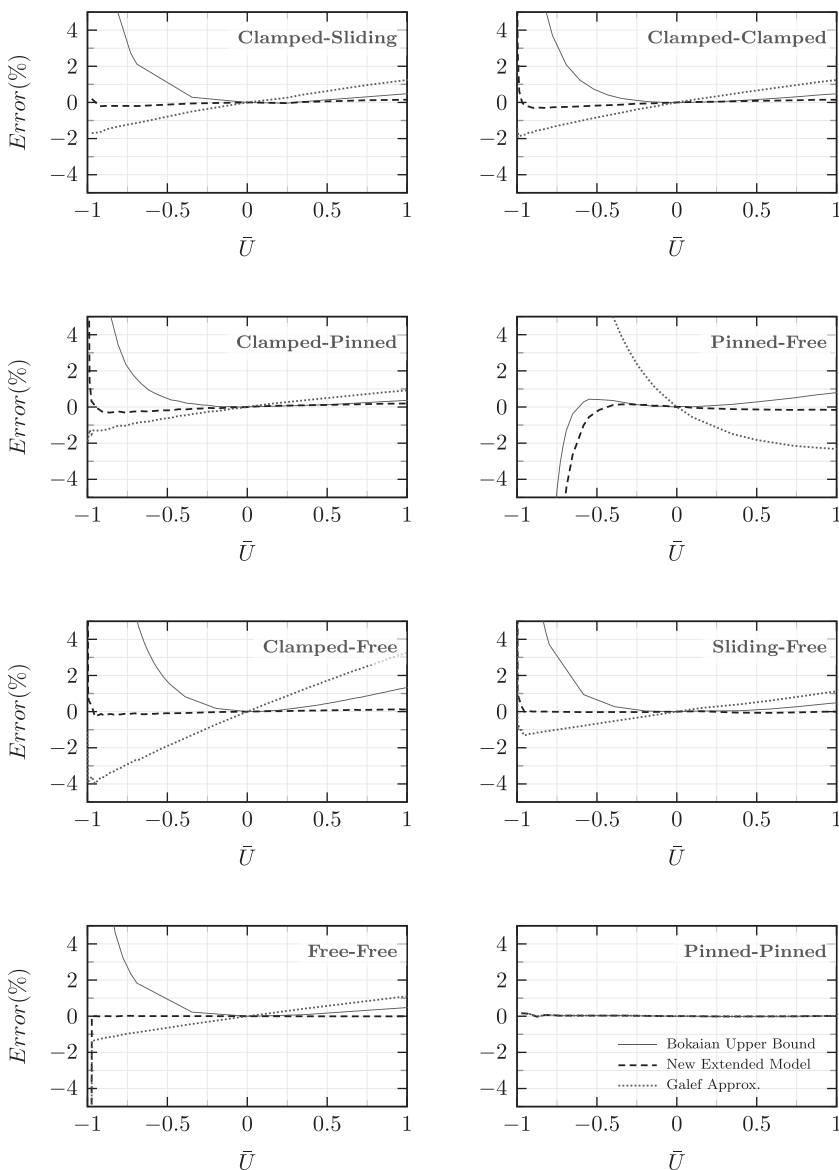


Fig. 5. Bokaian, new extended model and Galef deviations from numerical simulations for mode 1 and several end conditions as a function of normalized tension (\bar{U}), for small axial loads.

The axial loads were applied via temperature offsets. Modal analysis yielded the beam natural frequencies for the first 5 modes as a function of the applied axial load. The accuracy of the simulations is estimated in $\pm 0.05\%$, except very close to the buckling point, where it worsens and results in that area are treated with special care.

3.1. Analytical results

The coefficients of Eq. (10) for the fundamental mode were calculated analytically for the 8 end conditions considered. They are shown in Table 2. As shown in Section 2.6, the 3 coefficients are calculated using some parameters found in the literature that are also shown for convenience in Table 2.

The main objective of Table 2 is to compare the maximum deviation from the theoretical values for Eqs. (10), (6) and (8), which are our equation, Galef's and Bokaian's, respectively. Bokaian's equation is not applicable for compressive loads, especially close to the buckling point, so only the other two are compared in that region. In the region ($-1 < \bar{U} < 1$), Eq. (10) provided an accuracy close to the numerical precision ($\pm 0.05\%$). This means improvements of an order of magnitude or better with respect to Galef's equation.

For the positive axial load region ($0 < \bar{U} < \infty$) our equation also performed very well compared to Bokaian's Eq. (8). In our opinion, it is remarkable that it provided an accuracy around 0.1% for the free-free and sliding-free cases. This means two orders of magnitude better than Bokaian's equation.

Unfortunately, condition 3 does not work with higher modes. The reason is that Eq. (10) does not work well when the axial load is more negative than the buckling load of mode 1. As a consequence, only analytical results for the fundamental mode are given in Table 2. This is also the reason why the pinned-free case cannot be calculated analytically; it is equivalent to mode 2 of the free-free case, as shown in Table 1. The strange behavior of the pinned-free case is also briefly discussed in [4], and this equivalency is an alternative way to look at it.

3.2. Numerical results

The parameters γ , α and β from Eq. (10) were calculated by fitting the model to the obtained frequency-load curves. The resulting parameter values are displayed in Table A.3 for each mode and type of end conditions. Also, maximum deviation of Eq. (10) from numerical simulations is given for each case. Eqs. (14) and (15) were used to calculate the error at $\bar{U} = \infty$, where applicable. The range of tested axial loads was,

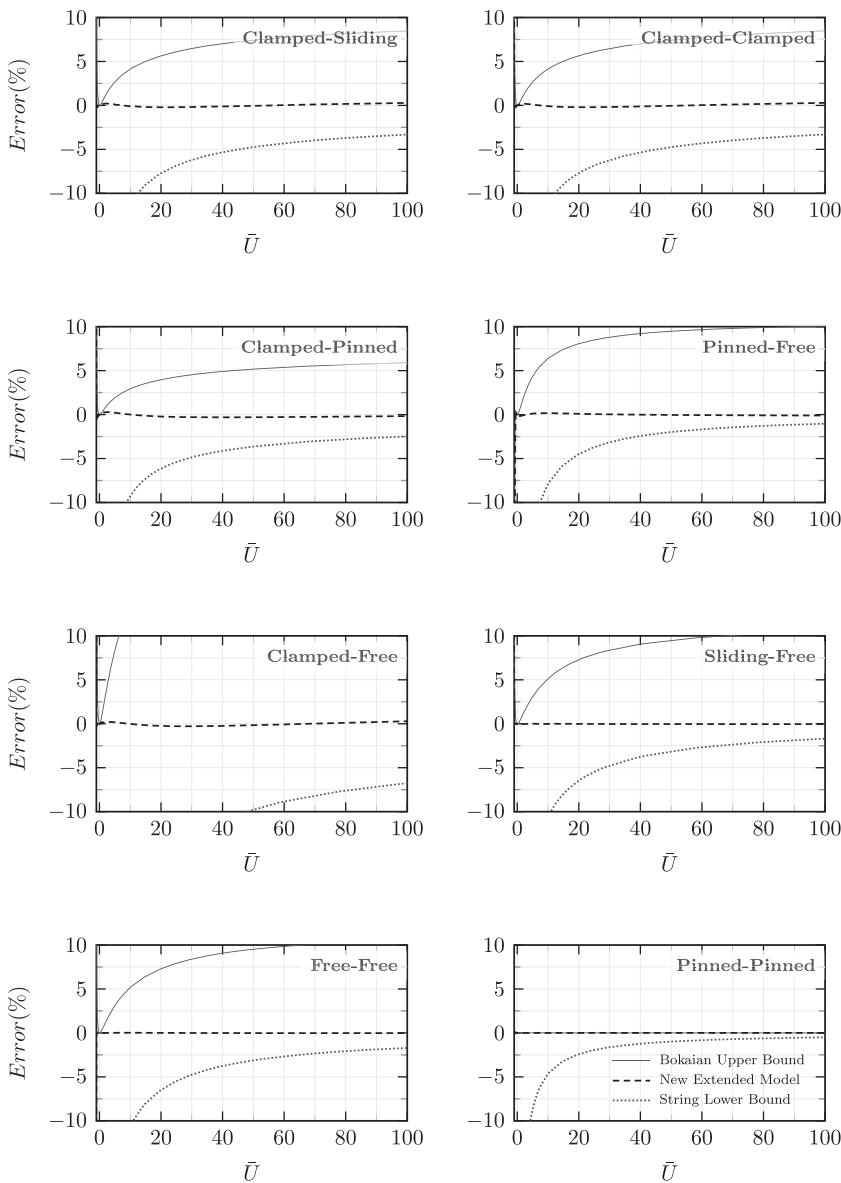


Fig. 6. Bokaian, new extended model and Galef's deviations from numerical simulations for mode 1 and several end conditions as a function of normalized tension (\bar{U}), for large axial loads.

at least, $-1 < \bar{U} < 100$ for the fundamental mode. For higher modes the error is given only down to the buckling axial load of mode 1 which, for the clamped-sliding case, for example, corresponds to $\bar{U} = -1/4$. As explained at the end of the previous section, the behavior of higher modes under more compressive axial loads than the buckling load of mode 1 is not well described by our equation. In addition, mode 1 of the pinned-free case is atypical given that the behavior in the region $(-1.0 < \bar{U} < -0.5)$ is qualitatively different from the other cases and not well described by any of the studied equations (Galef's, Bokaian's and ours). As a consequence, only the error when $-0.5 < \bar{U}$ is given in the pinned-free case.

The first mode data for $\bar{U} > 0$ was plotted in Fig. 4. It gives a good general comparison between numerical simulations, Bokaian closed-form equation, the tensioned-string limit and the new closed-form equation presented in this work. The solid line above and below the numerical simulation data are the Bokaian upper bound and the tensioned-string (no flexural stiffness) lower bounds, respectively. For comparison purposes Fig. 4 has the same format as figure 13 in Bokaian's paper [4]. For the clamped-free case, Bokaian's equation accuracy is significantly poorer than for the other cases, but the beam-to-string transition is still accurately modeled by our Eq. (11).

The accuracy of Galef's, Bokaian's and our equation for the fundamental mode and eight boundary conditions is shown in Figs. 5 and 6, for small and large axial loads, respectively. Bokaian's equation error can be higher than 20% in the worst case scenario for $0 < \bar{U} < 100$ (see clamped-free case of Fig. 6). However, Table A.3 shows that the new extended model fits remarkably well the transition from one regime to the other, yielding errors smaller than 0.36% in the worst case scenario for $-1 < \bar{U} < 100$. Note that this also includes compressive axial loads. In general, the error for mode 3 and higher is very small, similar to simulation precision when $\bar{U} < 100$. In addition, the γ and α values converge to 1 and 0, respectively, the higher the mode. This confirms Bokaian's statements that "the effect of end constraints on natural frequency is significant only in the first two modes", and "for higher modes the equation $\bar{\Omega} = \sqrt{1 + \bar{U}}$ may be used for all beams". For this reason, only the errors for the first two modes are plotted in Figs. 5–8.

Remarkably, the error is smaller than 0.08% for the fundamental mode in the free-free and sliding-free cases, and considering the full range $(-1 < U < \infty)$. Therefore, the extended model yields a near exact closed-form solution of the transcendental equation that arises from Eq. (2) for obtaining the resonant frequency (see Appendix B). Given that no accurate explicit closed-form solution existed, the transcen-

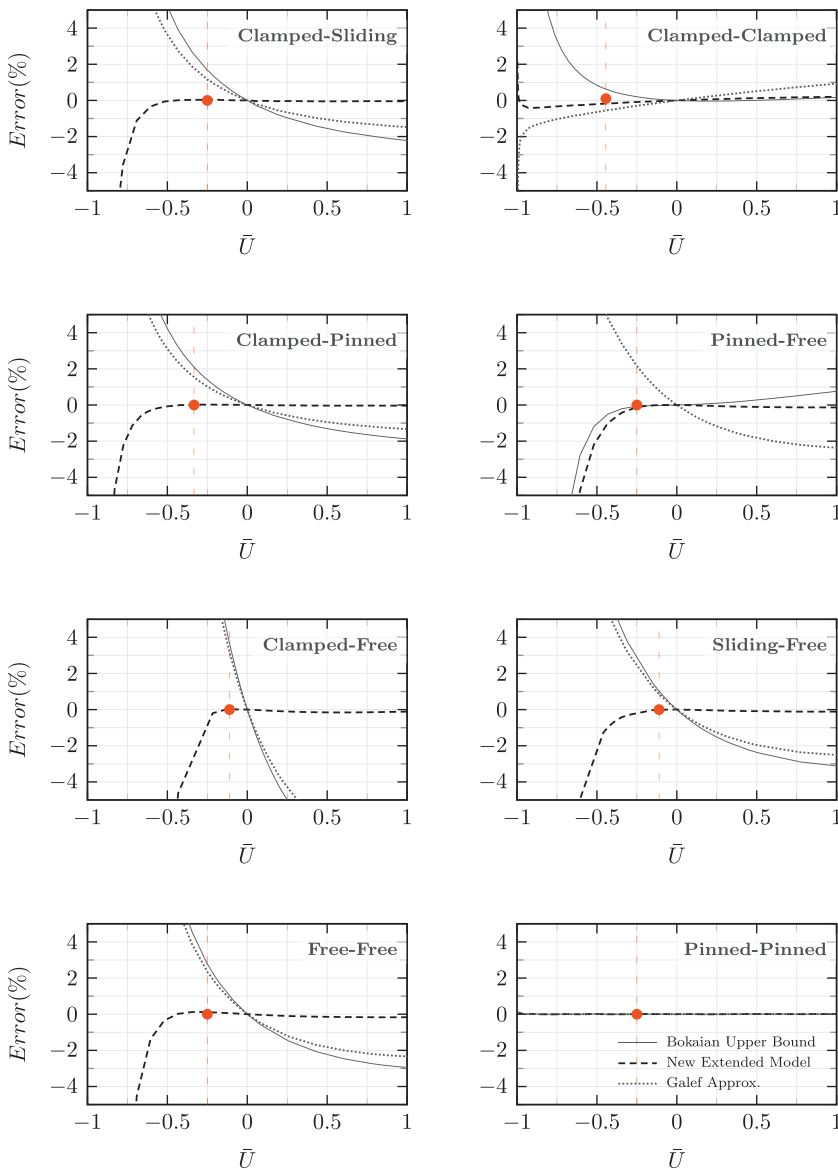


Fig. 7. Bokaian, new extended model and Galef deviations from numerical simulations for mode 2 and several end conditions as a function of normalized tension (\bar{U}), for small axial loads. Note that the New Extended Model is very accurate down to the buckling load of mode 1 (indicated with a vertical line and a dot), which can be found in Table A.3. (For interpretation of the references to color in this figure legend, the reader is referred to the web version of this article.)

dental equation had to be solved numerically in [10] for the free-free case.

For the fundamental mode, Galef’s equation showed an approximately linear error relationship with the compressive load (see Figs. 5 and 6), achieving errors typically larger than 1–2% near the buckling region ($\bar{U} \rightarrow -1$). The New Extended Model yielded a significantly better accuracy than Galef’s equation as Fig. 5 shows. Figs. 7 and 8 show the error for axial loads in the second mode. Again, in this case, the accuracy improvement for mode 2 is very significant for compressive loads, when compared with either Bokaian’s or Galef’s closed-form equations.

Table A.3 shows the optimized values for the three parameters of the new extended model (γ , β and α). Note that our equation has only two independent parameters if condition 1 (string limit) from Section 2.6 is applied to the higher modes. For the fundamental mode, any or all of the 3 conditions may be applied to reduce the number of independent parameters.

Finally, it is interesting to note that the parameters α , β and γ in Table A.3 are identical in the equivalent cases shown in Table 1. The optimization yielded very similar although not identical parameters which is attributable to the numerical precision of the simulations and the exact buckling load assumed. In these cases the 3 parameters were tweaked

so they were coincident for the sake of consistency. The maximum error is obviously given for the final tweaked parameters shown in the table.

4. Conclusion

No known exact closed-form solution relates the natural frequencies of beams under general boundary conditions with the applied tension. Some approximate equations proposed in the literature have been discussed. Some work reasonably well for small axial loads [1,4,10], but the error can be higher than 10% for medium and large axial loads or compressive ones which are not necessarily close to the buckling point. Others are only applicable for tensile or relatively large axial loads [15–19]. Some very useful but also relatively complex methodologies have been proposed in the literature to analyze even more complicated systems. They show how to find the associated transcendental equation that relates axial load and resonance frequency, but ultimately it is only solvable numerically.

In this work, a new closed-form equation that models very accurately the natural frequencies of axially loaded beams with various end conditions as a function of the applied axial load was presented. It models accurately the beam-to-string transition of beams under axial tension.

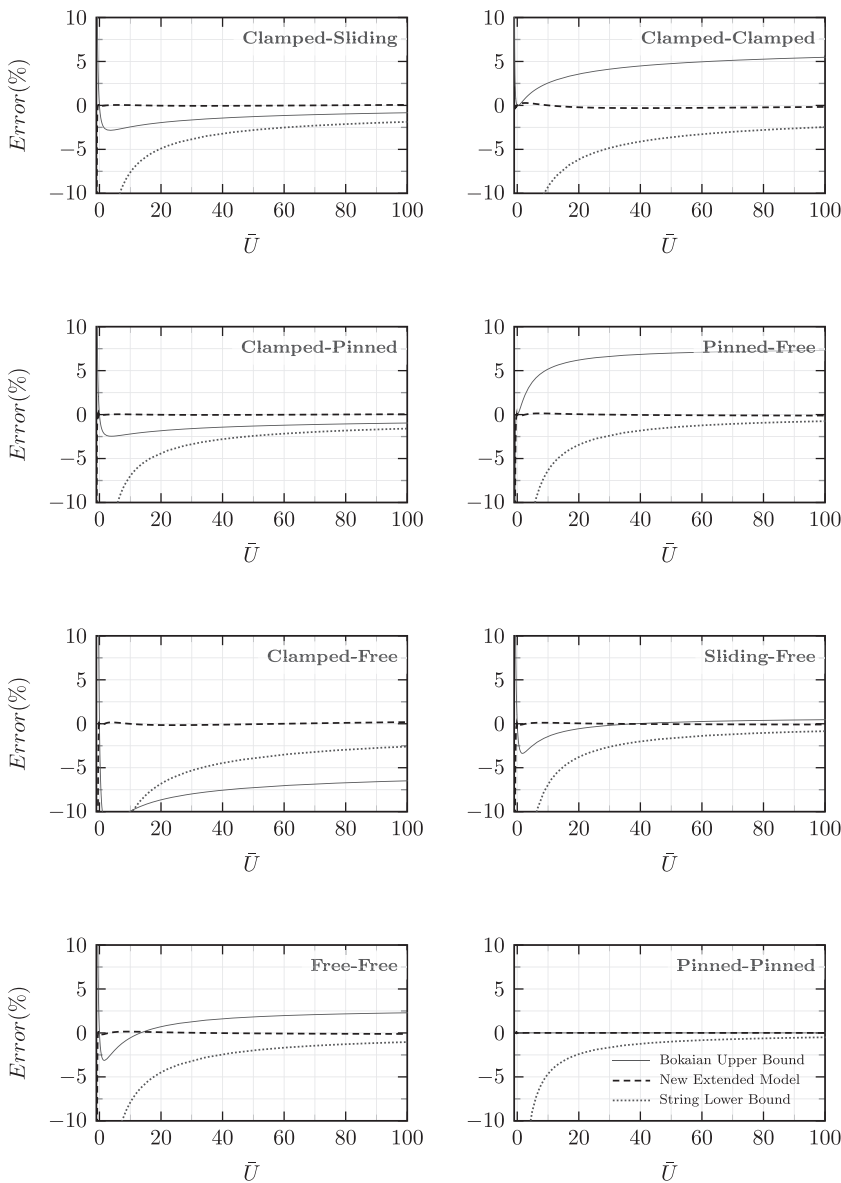


Fig. 8. Bokaian, new extended model and Galef deviations from numerical simulations for mode 2 and several end conditions as a function of normalized tension (\bar{U}), for large axial loads.

To best of the authors’ knowledge, it is the first closed-form in the literature that is very accurate in the full range of axial loads; from the buckling load of the fundamental mode to the string limit regime. Its accuracy was compared to two well-known simple closed-form equations, achieving improvements better than one order of magnitude for medium and large axial loads in the fundamental resonant mode. Similar improvements were achieved for compressive loads, which were more evident the closer to the buckling point in all cases, except in the pinned-free compressive case. It was shown that this later case is equivalent to the second mode of the free-free case.

The new closed-form is invariant for cases which are symmetrically equivalent, like the fundamental modes of the clamped-clamped and clamped-sliding cases, for example. This was confirmed with numerical simulations.

Remarkably, for the free-free and sliding-free cases, the accuracy of the new closed-form equation is within 0.08%, even when the axial load is close to the buckling point or in the string-limit regime. For the free-free and sliding-free cases, it is a near exact solution of the transcendental equation that describes the relationship between applied axial load and resonance frequency of axially loaded beams. For this reason, the equation proposed herein may be used for solving analytically and

yet very accurately, similar transcendental equations in other areas of study.

The new closed-form equation may also be used to accurately estimate the tension from the resonance frequency, or the propagation speed with the beam tension. It is well suited for studying long beams that may or not be strongly tensioned or compressed, as nanotubes.

Interestingly, the presented closed-form equation describes the resonance of a simple spring-mass model formed by three springs in parallel, where one of them can be decomposed into two springs in series. Therefore, it provides a very simple but accurate lumped method to model axially loaded beams. Potentially, it may be used for lumped modeling of more complex axially loaded cases, like elastic supports, inhomogeneous beams, harmonic vibrations, or maybe other structures like plates or membranes.





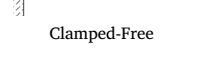


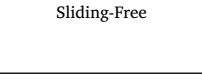
Acknowledgment

This work was supported by the Spanish [Ministerio de Economía y Competitividad](#) under Project [TEC2015-67278-R](#) and the [European Social Fund](#) (ESF), grant number [TEC2015-67278-R](#).

Appendix A. Table with γ , α and β values

Table A.3

For modes $i > 1$, the minimum considered \bar{U} is the one at which the beam buckles in the fundamental mode.

Mode	Number	\bar{P}_{cr}	Parameters			Max Error	Range
			γ	α	β		
	1	1	0.81626	0.19514	1.2114	0.29%	$-1.0 < \bar{U} < 100$
	2	8.18/4 ^a	0.85733	0.14757	1.1507	0.30%	$-4/8.18 < \bar{U} < 450$
	3	16/4	0.97881	0.08837	0.99648	0.06%	$-4/8.18 < \bar{U} < 100$
	4	25/4	0.99070	0.06783	0.82800	0.04%	$-4/8.18 < \bar{U} < 100$
	5	36/4	0.99561	0.05536	0.73791	0.06%	$-4/8.18 < \bar{U} < 100$
	1	1/4	0.81626	0.19514	1.2114	0.29%	$-1.0 < \bar{U} < 100$
	2	4/4	0.97881	0.08837	0.99648	0.05%	$-1/4 < \bar{U} < 100$
	3	9/4	0.99561	0.05536	0.73791	0.03%	$-1/4 < \bar{U} < 100$
	4	16/4	1.00050	0.04001	0.54600	0.02%	$-1/4 < \bar{U} < 100$
	5	25/4	1.00190	0.03140	0.44052	0.02%	$-1/4 < \bar{U} < 100$
	1	2.0457/4	0.85733	0.14757	1.1507	0.30%	$-1.0 < \bar{U} < 450$
	2	25/16	0.99070	0.06783	0.82800	0.04%	$-1/3 < \bar{U} < 100$
	3	49/16	0.99899	0.04646	0.61473	0.03%	$-1/3 < \bar{U} < 100$
	4	81/16	1.00140	0.03514	0.48438	0.02%	$-1/3 < \bar{U} < 100$
	5	121/16	1.00220	0.02831	0.40235	0.01%	$-1/3 < \bar{U} < 100$
	1	1/4	1	0	N/A	0.05%	$-1.0 < \bar{U} < 100$
	2	4/4	1	0	N/A	0.01%	$-1/4 < \bar{U} < 100$
	3	9/4	1	0	N/A	0.01%	$-1/4 < \bar{U} < 100$
	4	16/4	1	0	N/A	0.01%	$-1/4 < \bar{U} < 100$
	5	25/4	1	0	N/A	0.00%	$-1/4 < \bar{U} < 100$
	1	1/16	0.53471	0.74140	2.68280	0.29%	$-1.0 < \bar{U} < 100$
	2	9/16	1.04910	0.40695	1.59240	0.16%	$-1/9 < \bar{U} < 100$
	3	25/16	1.01940	0.23466	0.88952	0.10%	$-1/9 < \bar{U} < 100$
	4	49/16	1.01420	0.16932	0.61819	0.08%	$-1/9 < \bar{U} < 100$
	5	81/16	1.01120	0.13240	0.46908	0.06%	$-1/9 < \bar{U} < 100$
	1	1/4	0.77902	0.25234	1.7832	0.08%	$-1.0 < \bar{U} < \infty$
	2	4/4	0.91866	0.22018	1.11100	0.36%	$-1/4 < \bar{U} < \infty$
	3	9/4	0.95717	0.18546	0.73617	0.17%	$-1/4 < \bar{U} < \infty$
	4	16/4	0.97230	0.15508	0.59057	0.33%	$-1/4 < \bar{U} < \infty$
	5	25/4	0.98009	0.13343	0.49241	0.35%	$-1/4 < \bar{U} < \infty$
	1	1/4	0.91866	0.22018	1.11100	0.36%	$-1/2 < \bar{U} < \infty$
	2	4/4	0.97230	0.15508	0.59057	0.33%	$-1/4 < \bar{U} < \infty$
	3	9/4	0.98566	0.11700	0.40589	0.26%	$-1/4 < \bar{U} < \infty$
	4	16/4	0.99059	0.09253	0.31916	0.26%	$-1/4 < \bar{U} < \infty$
	5	25/4	0.99294	0.07740	0.26316	0.25%	$-1/4 < \bar{U} < \infty$
	1	1/16	0.77902	0.25234	1.7832	0.08%	$-1.0 < \bar{U} < \infty$
	2	9/16	0.95717	0.18546	0.73617	0.25%	$-1/9 < \bar{U} < \infty$
	3	25/16	0.98009	0.13343	0.49241	0.35%	$-1/9 < \bar{U} < \infty$
	4	49/16	0.99007	0.11112	0.30205	0.11%	$-1/9 < \bar{U} < \infty$
	5	81/16	0.99308	0.08984	0.24794	0.14%	$-1/9 < \bar{U} < \infty$

^a The critical load values for mode 2 is 9/4, according to [4]. However, simulations show it is 8.18/4 approximately, which is the value used in this work.

Appendix B. Transcendental characteristic equation of a free-free beam

The transverse vibrations of a beam under axial tension or compression is described by Eq. (2). The relationship between applied tension and resonance frequency can be obtained from this equation after solving the associated characteristic/frequency equation. Unfortunately, it is generally transcendental and therefore analytical solutions are not available and numerical procedures are required. The free-free case is one example where the analytical solution is not available. However, Eq. (10) or, equivalently, (11) work remarkably well as an approximate solution. For this reason, we feel it is appropriate to show the transcendental characteristic equation of a free-free beam [2,10] explicitly:

$$2\beta^6 [1 - \cosh(\alpha_1) \cos(\alpha_2)] + (\alpha_2^6 - \alpha_1^6) \sinh(\alpha_1) \sin(\alpha_2) = 0 \tag{B.1}$$

where:

$$\alpha_1 = \left(\frac{k^2}{2} + \sqrt{\frac{k^4}{4} + \beta^4} \right)^{1/2} \quad \alpha_2 = \left(-\frac{k^2}{2} + \sqrt{\frac{k^4}{4} + \beta^4} \right)^{1/2} \tag{B.2}$$

$$k^2 = \frac{TL^2}{EI} \quad \beta^4 = \frac{\rho A \omega^2 L^4}{EI} \tag{B.3}$$

Appendix C. List of symbols

A	Cross-sectional area
L	Beam length
ρ	Density, mass per volume
σ	Axial stress
T	Axial tensile force, $T = \sigma A$
E	Young's modulus
I	Second moment of area
x	Longitudinal coordinate, distance from left end of the beam
$Y(x)$	Beam deflection
Y_{max}	Maximum beam vibration along beam length
\bar{Y}	Normalized vibration amplitude, $Y(x)/Y_{max}$
α	Dimensionless parameter, $\sqrt{EI/(\rho A)}$
U	Dimensionless tension parameter, $TL^2/2EI$
U_{mi}	Dimensionless critical buckling load for vibration mode i (see Table 1 in[4])
\bar{U}	Normalized tension parameter for mode i , $U/U_{mi} = T/P_{cr}^i$
f	Natural frequency of beam = $\omega/2\pi$
f_0	Natural frequency of beam under no axial force = $\omega_0/2\pi$
$\bar{\Omega}$	Normalized natural frequency parameter, f/f_0
P_{cr}^i	Critical buckling load for mode i
\bar{P}_{cr}^i	Normalized critical buckling load for mode i , P_{cr}^i/P_{cr}^{c-c} , where $P_{cr}^{c-c} = 4\pi^2 EI/L^2$

References

- [1] Galef A. Bending frequencies of compressed beams. *J Acoust Soc Am* 1968;44(2):643.
- [2] Shaker FJ. Effect of axial load on mode shapes and frequencies of beams. NASA Lewis Research Centre Report NASA-TN-8109; 1975.
- [3] Bokaian A. Natural frequencies of beams under compressive axial loads. *J Sound Vib* 1988;126(1):49–65.
- [4] Bokaian A. Natural frequencies of beams under tensile axial loads. *J Sound Vib* 1990;142(3):481–98.
- [5] Guédé Z, Elishakoff I. Apparently first closed-form solutions for inhomogeneous vibrating beams under axial loading. In: Proceedings of the royal society of London A: mathematical, physical and engineering sciences, 457. The Royal Society; 2001. p. 623–49.
- [6] Joshi A, Suryanarayan S. Unified analytical solution for various boundary conditions for the coupled flexural-torsional vibration of beams subjected to axial loads and end moments. *J Sound Vib* 1989;129(2):313–26.
- [7] Stephen NG. Beam vibration under compressive axial load - upper and lower bound approximation. *J Sound Vib* 1989;131:345–50.
- [8] Gellert M, Gluck J. The influence of axial load on Eigen-frequencies of a vibrating lateral restraint cantilever. *Int J Mech Sci* 1972;14(11):723–8.
- [9] Abramovich H. Natural frequencies of timoshenko beams under compressive axial loads. *J Sound Vib* 1992;157:183–9.
- [10] Liu X, Ertekin R, Riggs H. Vibration of a free-free beam under tensile axial loads. *J Sound Vib* 1996;190:273–82.
- [11] Virgin LN. Vibration of axially-loaded structures. Cambridge University Press; 2007.
- [12] Yesilce Y, Demirdag O. Effect of axial force on free vibration of timoshenko multi-span beam carrying multiple spring-mass systems. *Int J Mech Sci* 2008;50(6):995–1003.
- [13] Carpinteri A, Malvano R, Manuella A, Piana G. Fundamental frequency evolution in slender beams subjected to imposed axial displacements. *J Sound Vib* 2014;333(11):2390–403.
- [14] Burlon A, Failla G, Arena F. Exact frequency response analysis of axially loaded beams with viscoelastic dampers. *Int J Mech Sci* 2016;115–116:370–84.
- [15] Zui H, Shinke T, Namita Y. Practical formulas for estimation of cable tension by vibration method. *J Struct Eng* 1996;122(6):651–6.
- [16] Mehrabi AB, Tabatabai H. Unified finite difference formulation for free vibration of cables. *J Struct Eng* 1998;124(11):1313–22.
- [17] Ren W-X, Chen G, Hu W-H, et al. Empirical formulas to estimate cable tension by cable fundamental frequency. *Struct Eng Mech* 2005;20(3):363–80.
- [18] Fang Z, Wang J-q. Practical formula for cable tension estimation by vibration method. *J Bridge Eng* 2010;17(1):161–4.
- [19] Huang Y-H, Fu J-Y, Wang R-H, Gan Q, Liu A-R. Unified practical formulas for vibration-based method of cable tension estimation. *Adv Struct Eng* 2015;18(3):405–22.
- [20] Gillich G-R, Furdul H, Abdel Wahab M, Korke Z. A robust damage detection method based on multi-modal analysis in variable temperature conditions. *Mech Syst Signal Process* 2019;115:361–79.
- [21] Du X, Wang L, Li A, Wang L, Sun D. High accuracy resonant pressure sensor with balanced-mass def resonator and twinborn diaphragms. *J Microelectromech Syst* 2017;26(1):235–45.
- [22] Hou Z, Xiao D, Wu X, Dong P, Chen Z, Niu Z, et al. Effect of axial force on the performance of micromachined vibratory rate gyroscopes. *Sensors* 2010;11(1):296–309.
- [23] Hu Y, Xue H, Hu H. A piezoelectric power harvester with adjustable frequency through axial preloads. *Smart Mater Struct* 2007;16(5):1961.
- [24] Soma A, Ballestra A. Residual stress measurement method in mems microbeams using frequency shift data. *J Micromech Microeng* 2009;19(9):095023.
- [25] Blevins RD, Plunkett R. Formulas for natural frequency and mode shape. *J Appl Mech* 1980;47:461.
- [26] Wei X, Chen Q, Xu S, Peng L, Zuo J. Beam to string transition of vibrating carbon nanotubes under axial tension. *Adv Funct Mater* 2009;19(11):1753–8.
- [27] Wittrick W. Some observations on the dynamic equations of prismatic members in compression. *Int J Mech Sci* 1985;27(6):375–82.
- [28] Casas JR. A combined method for measuring cable forces: the cable-stayed alamillo bridge, Spain. *Struct Eng Int* 1994;4(4):235–40.
- [29] Chen L-W, Shen G-S. Vibration and buckling of initially stressed curved beams. *J Sound Vib* 1998;215(3):511–26.
- [30] Joshi A, Suryanarayan S. Coupled flexural-torsional vibration of beams in the presence of static axial loads and end moments. *J Sound Vib* 1984;92(4):583–9.
- [31] Ni Z, Hua H. Axial-bending coupled vibration analysis of an axially-loaded stepped multi-layered beam with arbitrary boundary conditions. *Int J Mech Sci* 2018;138–139:187–98.
- [32] Naguleswaran S. Transverse vibration of a uniform euler-bernuulli beam under linearly varying axial force. *J Sound Vib* 2004;275(1–2):47–57.
- [33] Li X, Tang A, Xi L. Vibration of a rayleigh cantilever beam with axial force and tip mass. *J Constr Steel Res* 2013;80:15–22.
- [34] Kim P, Bae S, Seok J. Resonant behaviors of a nonlinear cantilever beam with tip mass subject to an axial force and electrostatic excitation. *Int J Mech Sci* 2012;64(1):232–57.
- [35] Yang J, Chen Y, Xiang Y, Jia X. Free and forced vibration of cracked inhomogeneous beams under an axial force and a moving load. *J Sound Vib* 2008;312(1–2):166–81.
- [36] Mei C, Karpenko Y, Moody S, Allen D. Analytical approach to free and forced vibrations of axially loaded cracked timoshenko beams. *J Sound Vib* 2006;291(3):1041–60.
- [37] Binici B. Vibration of beams with multiple open cracks subjected to axial force. *J Sound Vib* 2005;287(1–2):277–95.
- [38] Aydin K. Vibratory characteristics of euler-bernuulli beams with an arbitrary number of cracks subjected to axial load. *J Vib Control* 2008;14(4):485–510.
- [39] Caddemi S, Calio I. The influence of the axial force on the vibration of the euler-bernuulli beam with an arbitrary number of cracks. *Arch Appl Mech* 2012;82(6):827–39.
- [40] Arboleda-Monsalve LG, Zapata-Medina DG, Aristizabal-Ochoa JD. Stability and natural frequencies of a weakened timoshenko beam-column with generalized end conditions under constant axial load. *J Sound Vib* 2007;307(1–2):89–112.
- [41] Treysede F. Vibration analysis of horizontal self-weighted beams and cables with bending stiffness subjected to thermal loads. *J Sound Vib* 2010;329(9):1536–52.
- [42] Farghaly S, El-Sayed T. Exact free vibration of multi-step timoshenko beam system with several attachments. *Mech Syst Signal Process* 2016;72:525–46.
- [43] Hijmissen J, Van den Heuvel N, Van Horsen W. On the effect of the bending stiffness on the damping properties of a tensioned cable with an attached tuned-mass-damper. *Eng Struct* 2009;31(5):1276–85.
- [44] Impollonia N, Ricciardi G, Saitta F. Dynamic behavior of stay cables with rotational dampers. *J Eng Mech* 2009;136(6):697–709.
- [45] Virgin L, Plaut R. Effect of axial load on forced vibrations of beams. *J Sound Vib* 1993;168(3):395–405.
- [46] Chen Z, Yang Z, Guo N, Zhang G. An energy finite element method for high frequency vibration analysis of beams with axial force. *Appl Math Model* 2018;61:521–39.
- [47] Zhang Y, Lu Y, Ma G. Effect of compressive axial load on forced transverse vibrations of a double-beam system. *Int J Mech Sci* 2008;50(2):299–305.
- [48] Mazzilli CE, Sanches CT, Neto OGB, Wiercigroch M, Keber M. Non-linear modal analysis for beams subjected to axial loads: analytical and finite-element solutions. *Int J Non Linear Mech* 2008;43(6):551–61.
- [49] Gunda JB, Gupta R, Janardhan GR, Rao GV. Large amplitude vibration analysis of composite beams: simple closed-form solutions. *Compos Struct* 2011;93(2):870–9.
- [50] Yang T, Wiebe R. Experimental study on the effect of large axial tensile force on the natural frequency of a fixed-fixed steel beam. In: *Nonlinear dynamics*, I. Springer; 2017. p. 127–34.
- [51] Li C, Lim CW, Yu J, Zeng Q. Analytical solutions for vibration of simply supported nonlocal nanobeams with an axial force. *Int J Struct Stab Dyn* 2011;11(02):257–71.
- [52] Caddemi S, Calio I. Exact closed-form solution for the vibration modes of the euler-bernuulli beam with multiple open cracks. *J Sound Vib* 2009;327(3):473–89.
- [53] Baek C-W, Kim Y-K, Ahn Y, Kim Y-H. Measurement of the mechanical properties of electroplated gold thin films using micromachined beam structures. *Sens Actuators A* 2005;117(1):17–27.
- [54] Meirovitch L. Analytical methods in vibrations, 438. Macmillan New York; 1967.